

Preparation and characterization of UV-cured acrylic nanocomposites based on modified organophilic montmorillonites

R. Peila · G. Malucelli · A. Priola

ICTAC2008 Conference
© Akadémiai Kiadó, Budapest, Hungary 2009

Abstract UV-cured nanocomposites have been prepared through the photopolymerization of the acrylic resin BEMA (Bisphenol A ethoxylate dimethacrylate) added with organophilic montmorillonites. Two types of commercially available nanoclays namely Cloisite 30B and Cloisite Na⁺ were further modified with organic compatibilizers (dodecylsuccinic anhydride, octadecylamine, octadecanoic alcohol and octadecanoic acid) in order to increase their basal spacing and improve the dispersion in the acrylic matrix. The modification with the organic compatibilizers determined an increase of the interlayer distance, as revealed by XRD (X-Ray Diffraction) analysis. The different types of the modified nanoclays were then dispersed in BEMA monomer at 5% m/m concentration and UV-cured in order to prepare the nanocomposites. XRD measurements performed on the nanocomposites showed a slight increase of the interlayer distance indicating the formation of intercalated structures. The photopolymerization reaction was monitored through real-time FT-IR (Fourier Transform Infrared Spectroscopy) in order to check any influence of the nanofillers on the cure kinetics. The nanocomposites were investigated by DSC (Differential Scanning Calorimetry) and TG (Thermogravimetric) analyses and compared to the neat UV-cured resin. The presence of the nanofillers did not influence the glass transition temperature (T_g) of the acrylic resin; in addition an increase of the thermal stability in air of the nanocomposites was evidenced through TG analysis.

Keywords Acrylic resin · Nanocomposites · Organo-montmorillonite · Thermal analysis · UV curing

Introduction

Naturally available layered silicate like montmorillonite have received great attention as reinforcing materials for polymers mainly thanks to their high aspect ratio, surface area and possibility of intercalated/exfoliated morphology. However, the high polarity of the nanoclays due to the presence of strong ionic bonds between the silicate layers and the intergallery cations makes difficult to obtain intercalated/exfoliated nanocomposites in apolar polymers. Thus, it becomes necessary to modify the structure of the nanoclays, i.e., by exchanging the alkaline cations with organic surfactants like alkyl ammonium or phosphonium quaternary ions, which make the nanoclays organophilic and improve the compatibility with the polymer matrix. If intercalated/exfoliated morphology are achieved, it is possible to obtain enhanced properties even at low concentrations (3–5% m/m) [1–4].

The nanocomposites are generally prepared either by incorporating the nanofillers into the molten polymer or by the in situ polymerization technique [5, 6]. As in situ polymerization, the UV curing technique represents an interesting possibility. This method uses UV irradiation to start the polymerization reaction of multifunctional monomers. It requires the presence of a suitable photoinitiator that interacts with the radiation, giving rise to the formation of free radicals or cations to interact with the monomer and start the curing reaction. The nanofillers are generally incorporated into the liquid monomer, subsequently added of a small amount of photoinitiator and then photopolymerized. Compared to other polymerization, the UV-curing allows a

R. Peila (✉) · G. Malucelli · A. Priola
Dipartimento di Scienza dei Materiali e Ingegneria Chimica,
Politecnico di Torino C.so Duca degli Abruzzi,
24-10129 Torino, Italy
e-mail: roberta.peila@polito.it

good control of the swelling to ensure the penetration of the resin in the intergallery region of the platelets; it is very fast and can be easily controlled adjusting the light intensity. In addition, it can be performed at ambient temperature and, being a solvent-free technique, is environmentally friendly. These advantages make this method very suitable for the synthesis of polymer thermoset nanocomposites [7–15].

In this study, we have prepared UV-cured nanocomposites based on two different types of montmorillonites, further modified with organic compatibilizers (dodecylsuccinic anhydride, octadecylamine, octadecanoic alcohol and octadecanoic acid). An acrylic resin (Bisphenol-A ethoxylate dimethacrylate, BEMA) was used as photocurable matrix. It was added of 5% m/m of the modified organophilic montmorillonites and subjected to the UV-curing process. The morphology of the obtained nanocomposites was investigated through XRD analysis, which evidenced the formation of intercalated structures.

The nanocomposites were thermally investigated by DSC and TG analyses.

Experimental

Materials

Two types of commercially available montmorillonite were used: Cloisite Na⁺ (Clo-Na) and Cloisite 30B (Clo-30B). They were purchased from Southern Clay Product Inc. (USA).

The CloNa was modified by ETHOQUAD (ETH) 0/12 (9-Octadecen-1-aminium, N,N-bis (2-hydroxyethyl)-N-methyl chloride) purchased from AKZO NOBEL. The obtained product was named Clo-ETH.

Dodecylsuccinic anhydride (DSA), octadecylamine (ODA), octadecanoic alcohol (ODOH) and octadecanoic acid (AcOD) were used as compatibilizers and were Aldrich products.

Bisphenol-A ethoxylate (15 EO/phenol) dimethacrylate (BEMA), from Aldrich, was used as photocurable matrix; it was added of 2-hydroxy-2-methyl-1-phenyl-1-propanone as photoinitiator, from CIBA.

Figure 1 shows the structure of the Clo-30B and Clo-Na modifiers together with the compatibilizers employed.

Nanoclays modification

Clo-Na was treated with ETH in order to exchange Na⁺ ions with ammonium quaternary ions. A 1% m/m dispersion of Clo-Na in deionized water was added of ETH using an excess of 20% with respect to the CEC (cations exchange capacity) of Clo-Na. The dispersion was stirred 24 h at 333K. The exchanged Clo-Na was washed with

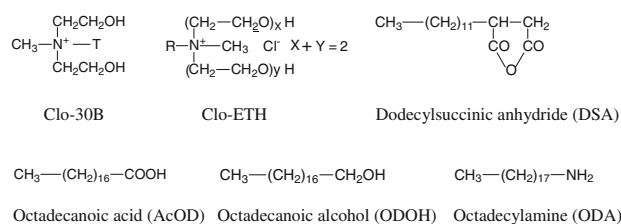


Fig. 1 Structure of the montmorillonite modifiers and compatibilizers used

fresh water, monitoring the disappearance of the chloride ions with AgNO₃ solution.

Clo-ETH and Clo-30B were afterward modified with the aforementioned organic compatibilizers. Five grams of the nanoclays were dispersed in 2,2-dimethoxyethane at 348K. A stoichiometric amount of each modifier with respect to the –OH groups of the modified nanoclays was added and the dispersion was kept for 2 h at 348K. It was then filtered and washed with fresh solvent and left in oven at 343K until constant dried mass was reached.

Some of the Clo-30B products modified with the described organic compatibilizers were previously used for the preparation of LDPE (low density polyethylene) nanocomposites [16].

Preparation of the UV-cured nanocomposites

The modified nanoclays were dispersed into the liquid BEMA monomer at a concentration of 5% m/m. The dispersions were kept in an ultrasonic bath (mod. Branson 1210) for 2 h at room temperature. The dispersions were then added of 4% m/m of photoinitiator and coated on polypropylene substrates (film thickness 100 μm). They were subsequently cured with a medium vapor pressure Hg UV lamp (Helios Italquartz) with a radiation intensity on the surface of the samples of 20 mW/cm². The samples were UV-cured in N₂ atmosphere.

Characterization techniques

The morphology of the modified nanoclays and of the UV-cured nanocomposites was studied through XRD analysis using a Philips X'Pert-MPD diffractometer (CuK_α radiation). Two 2θ ranges were analysed: 2 < 2θ < 30°, with 0.02 Δ2θ step and 2 s step time; 0.7 < 2θ < 10°, through wide angle X-ray scattering (WAXS) analysis, with 0.01 Δθ step and 20 s step time.

The cure kinetics was monitored by means of a Real-Time FT-IR, using a Thermo-Nicolet 5700 instrument. The liquid dispersions were placed on a silicon wafer and the samples were exposed simultaneously to the UV light to induce the photopolymerization and to the IR beam to analyze the extent of the reaction. The photopolymerization

was induced by a medium pressure Hg lamp equipped with an optical waveguide (light intensity on the surface of the sample of about 4 mW/cm^2). The decrease of the methacrylic absorption peak, in the $1,620\text{--}1,660 \text{ cm}^{-1}$ region, was continuously monitored and at the end of the analysis conversion versus irradiation time profiles were determined. The polymerization reactions were performed at room temperature and 25–30% RH (relative humidity).

The gel content (gel %) of the nanocomposites and of the neat UV-cured resin was evaluated by measuring the weight loss of the samples after 24 h extraction at room temperature with CHCl_3 .

The glass transition temperatures (T_g) of the samples were determined through differential scanning calorimetry (DSC) using a Mettler DSC 30 instrument, equipped with a low temperature probe, with a heating rate of 293K/min .

Thermogravimetric (TG) analyses were performed in air (flow rate of 60 ml/min) using a Mettler TGA-SDTA 851 instrument from room temperature to 1023K with a heating rate of 283K/min .

Results and discussions

Properties of the nanocomposites

The modified nanoclays were characterized through XRD analysis in order to determine the interlayer distance. The interlamellar basal spacing of the modified nanoclays and of the nanocomposites are shown in Table 1. A clear increase of the basal spacing d_{001} is evident for both the nanoclay systems after the treatment.

It can be noted that Clo-ETH has practically the same spacing of Clo-30B, in agreement with the similar structure. The interaction of Clo-ETH with the different compatibilizers indicates that only DSA gave rise to a strong increase of the basal spacing. This can be attributed to the reaction of the DSA succinic group with the OH of Clo-ETH.

As far as modified Clo-30B is concerned, Table 1 shows an average increase of the basal spacing of more than 20 \AA for all the compatibilizers. This behavior can be attributed to the different structure of the ammonium ion of Clo-ETH with respect to Clo-30B (Fig. 1).

The modified nanoclays were subsequently dispersed into the BEMA monomer. The dispersions were analyzed through XRD analysis both before and after the photopolymerization. No difference was observed for the interlamellar distance values of the liquid dispersions and of the nanocomposite. Therefore, the intercalation was achieved in the liquid dispersions and was maintained in the UV-cured nanocomposites. Thus only the interlamellar distances of the nanocomposites are reported in Table 1. Figures 2 and 3 report some typical XRD patterns of the same nanocomposites.

The nanocomposites based on the modified Clo-ETH showed Δd values similar to those obtained for the modified Clo-30B, indicating that BEMA monomer entered the nanoclay galleries in the same way.

In order to check the effect of the presence of the nanofillers on the photopolymerization kinetics, the UV-curing was followed by means of real time FT-IR technique, monitoring the decrease of the methacrylic absorption peak in the $1,620\text{--}1,660 \text{ cm}^{-1}$ region. The curing process was triggered by using a medium pressure Hg lamp equipped with an optical waveguide. The double bonds conversion as a function of the irradiation time for the neat resin and for the nanocomposites based on the modified Clo-ETH and Clo-30B are plotted in Figs. 4 and 5, respectively.

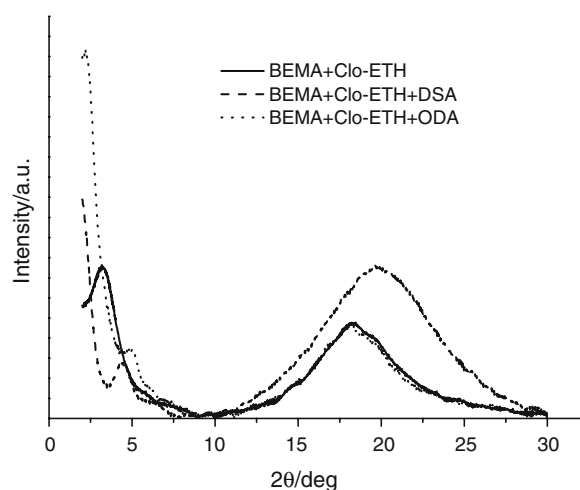


Fig. 2 XRD patterns of the nanocomposites based on the modified Clo-Na nanoclays

Table 1 d_{001} values of the modified nanoclays and nanocomposites

		+DSA	+ODA	+ODOH	+AcOD
Clo-Na	12.0	–	–	–	–
Clo-ETH	17.3	34.2 (16.9)	17.4 (0.1)	17.5 (0.2)	18.6 (1.3)
BEMA + Clo-ETH	30.4 (13.1)	43.5 (26.2)	39.9 (22.6)	35.2 (17.9)	36.3 (19.0)
Clo-30B	18.4	38.2 (19.8)	40.3 (21.9)	42.6 (24.2)	39.2 (20.8)
BEMA + Clo-30B	41.2 (22.8)	42.3 (23.9)	44.1 (25.7)	40.2 (21.8)	41.4 (23.0)

Unites: \AA ; in parenthesis Δd_{001} differences, calculated with respect to precursor Clo-ETH or Clo-30B nanoclay, are given

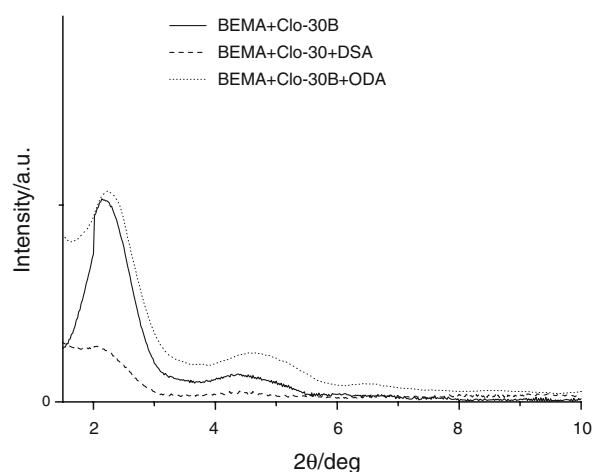


Fig. 3 XRD patterns of the nanocomposites based on the modified Clo-30B nanoclays

It can be noted that in any case the photopolymerization proceeded rapidly and reached the asymptotic value (between 95 and 100%) after about 10 s. The presence of 5% m/m of nanoclays in the UV-curable systems did not affect the curing rate as shown by the slope of the conversion curves. The maximum degree of conversion of the nanocomposites was slightly higher with respect to that of the neat resin. This may be attributed to some scattering phenomena due to the presence of the silicate platelets that interfered with the UV-light.

The T_g values of the nanocomposites, as determined by DSC analysis, are collected in Table 2. The obtained results indicated that all the nanocomposites exhibited the same T_g values, which are very close to that of the neat UV-cured BEMA resin. Therefore, we can conclude that the intercalation effect evidenced by XRD analysis did not influence the mobility of the polymer chains. In the same table, the

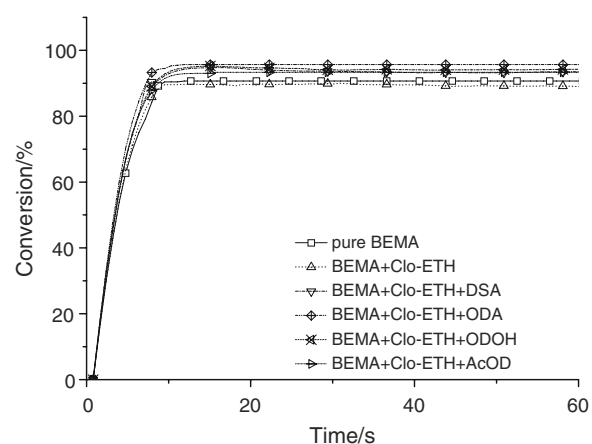


Fig. 4 RT-IR spectra of the UV-curable systems based on modified Clo-Na nanoclays

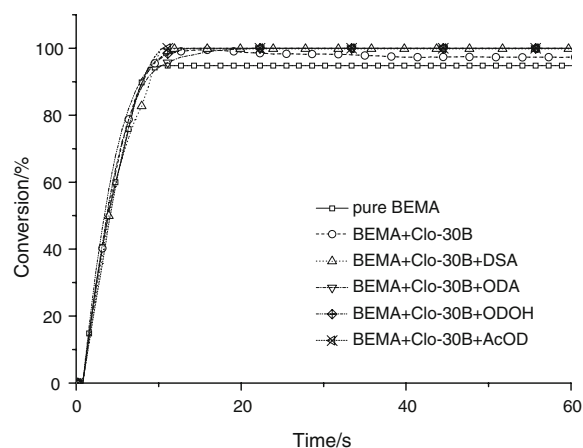


Fig. 5 RT-IR spectra of the UV-curable systems based on modified Clo-30B nanoclays

gel% values of the systems are reported. In any case high gel content (in between 94 and 98%) was achieved.

TG analysis

The thermogravimetric analysis performed in air on the nanoclay powders showed different steps of degradation for the modified and unmodified nanoparticles. The thermal degradation of the unmodified Clo-Na, in Fig. 6, shows one step of mass loss which is around 363K and is attributable to the loss of water molecules present in the interlayer region or on the surface of the nanoclays.

TG derivative curves related to the modified Clo-ETH and Clo-30B (Fig. 7) showed two main peaks of degradation at about 353K and 533K. This latter is due to the degradation of the organic modifiers. Although the origin of the step of degradation is not fully understood, according to Edwards [17] and to Leszczynska [18] it may be related to the diffusion of the compatibilizers and to changes in the pathway of degradation.

Table 2 Gel% and T_g values of the BEMA nanocomposites

Sample	T_g (K)	Gel (%)
Pure BEMA	231	95
BEMA + Clo-Na	230	94
BEMA + Clo-ETH	227	94
BEMA + Clo-ETH + DSA	227	95
BEMA + Clo-ETH + ODA	228	96
BEMA + Clo-ETH + ODOH	228	96
BEMA + Clo-ETH + AcOD	227	96
BEMA + Clo-30B	228	98
BEMA + Clo-30B + DSA	227	98
BEMA + Clo-30B + ODA	227	97
BEMA + Clo-30B + AcOD	227	98
BEMA + Clo-30B + ODOH	228	97

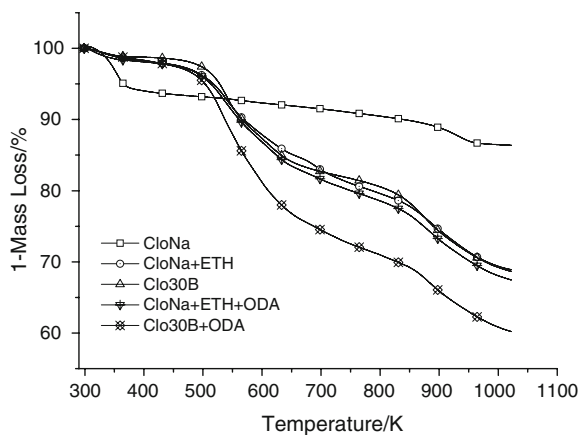


Fig. 6 Thermal degradation curves of the unmodified and modified nanoclays

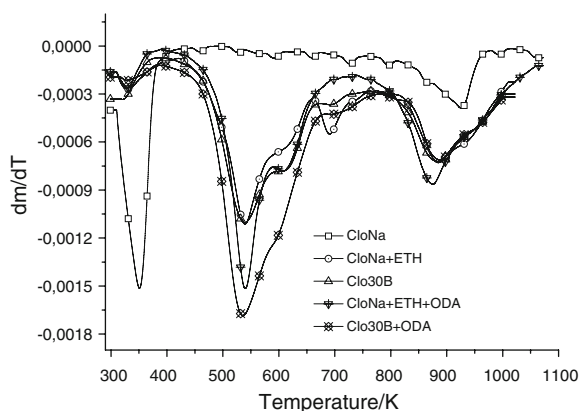


Fig. 7 Derivatives of the thermal degradation curves of the unmodified and modified nanoclays

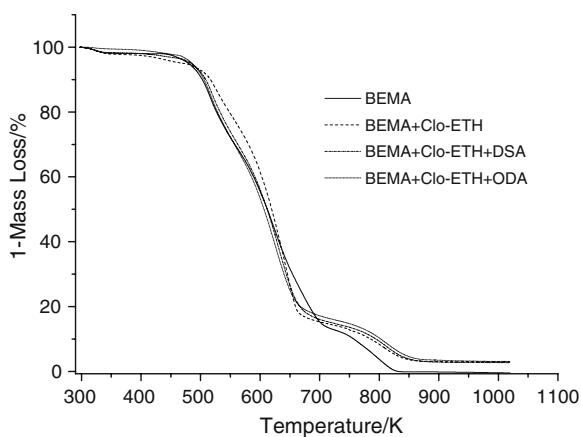


Fig. 8 TG curves in air of the BEMA nanocomposites based on the modified Clo-Na nanoclays

In Fig. 8, the TG curves of the BEMA nanocomposites based on the modified Clo-Na are reported. Three degradation steps are detectable from the obtained curves. The first step is attributable to the loss of water in the region

Table 3 Thermal stability of the BEMA nanocomposites

Sample	T10 (K)	T50 (K)	Char content (%)
Pure BEMA	503	613	0
BEMA + Clo-Na	505	613	4.7
BEMA + Clo-ETH	517	620	3.8
BEMA + Clo-ETH + DSA	509	612	3.4
BEMA + Clo-ETH + ODOH	510	605	3.3
BEMA + Clo-ETH + AcOD	501	592	3.3
BEMA + Clo-ETH + ODA	510	607	3.2
BEMA + Clo-30B	511	605	3.8
BEMA + Clo-30B + DSA	516	616	3.3
BEMA + Clo-30B + ODA	516	607	3.2
BEMA + Clo-30B + AcOD	505	605	3.4
BEMA + Clo-30B + ODOH	515	606	3.3

around 363K; in the range of temperatures between 473K and 673K the main degradation step of the polymeric material was observed. The final step around 773K is due to the reaction of the pyrolysis products with the oxygen. In Table 3, the temperatures corresponding to a mass loss of 10% (T10) and 50% (T50) of the nanocomposites are collected together with the char content. In any case, the presence of the modified nanoclays slightly improved the thermal stability in air of BEMA in terms of temperature of initial degradation (T10). The char values are in agreement with the pure silicate content of the nanoclays.

Figure 9 shows the TG curves in air of the BEMA nanocomposites based on the modified Clo-30B nanoclays. The T10 and T50 together with the char content are collected in Table 3. A similar type of thermal degradation behaviour as observed for the modified Clo-Na nanocomposites is evident, although slightly higher T10 values were obtained. This could be related to the higher intercalation values of such nanocomposites, as reported in Table 1.

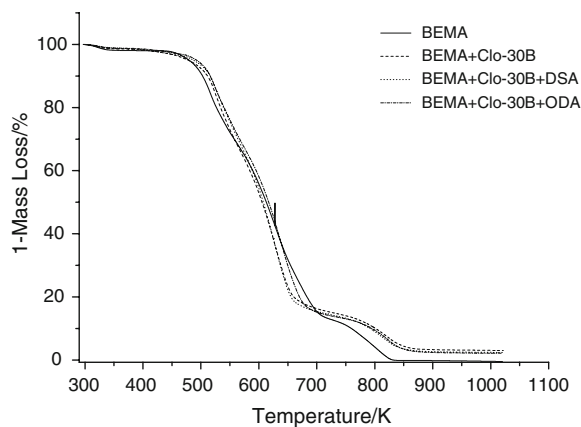


Fig. 9 TG curves in air of the BEMA nanocomposites based on the modified Clo-30B nanoclays

Conclusions

The preparation of nanocomposites via photopolymerization of dispersions of organophilic modified montmorillonites in an acrylic resin was investigated. Different organic compatibilizers (dodecylsuccinic anhydride, octadecylamine, octadecanoic alcohol and octadecanoic acid) were used as modifiers of two types of commercially available nanoclays, namely Cloisite 30B and Cloisite Na⁺. An increase of their basal spacing, as revealed by XRD analysis, was achieved. The modified nanoclays were then dispersed in the acrylic resin at 5% m/m concentration and UV-cured. The conversion versus time profile showed that the presence of the nanoclays did not affect the curing rate and the final conversion of the acrylic double bonds. XRD measurements performed on the nanocomposites showed a slight increase of the interlayer distance indicating the formation of intercalated structures. DSC analysis evidenced that the T_g of the nanocomposites did not change with respect to the neat UV-cured resin in the presence of 5% m/m of the nanofillers. TG analysis in air showed a slight increase of the initial thermal degradation temperatures of the nanocomposites.

Acknowledgements The final support of Regional Project (Piedmont D26 2004) is gratefully acknowledged.

References

- Kumar AP, Depan D, Tomer N, Singh RP. Nanoscale particles for polymer degradation and stabilization—trends and future perspectives. *Prog Polym Sci.* 2009;34:479–515.
- Pavlidou S, Papaspyrides CD. A review on polymer-layered silicate nanocomposites. *Prog Polym Sci.* 2008;33:1119–98.
- Zidkheir B, Abdelgoad M. Effect of surfactant agent upon the structure of montmorillonite. *J Therm Anal Cal.* 2008;94:181–7.
- Ray SS, Okamoto M. Polymer/layered silicate nanocomposites: a review from preparation to processing. *Prog Polym Sci.* 2003;28:1539–641.
- Rozenberg BA, Tenne R. Polymer-assisted fabrication of nanoparticles and nanocomposites. *Prog Polym Sci.* 2008;33:40–112.
- Karasu F, Aydin M, Kaya MA, Balta DK, Arsu N. Determination of photoinitiated polymerisation of multifunctional acrylates with acetic acid derivatives of thioxanthone by RT-FTIR. *Prog Org Coat.* 2009;64:1–4.
- Rozenberg BA, Tenne R. Polymer-assisted fabrication of nanoparticles and nanocomposites. *Prog Polym Sci.* 2008;33:40–112.
- Decker C, Keller L, Zahouily K, Benfarhi S. Synthesis of nanocomposite polymers by UV-radiation curing. *Polymer.* 2005;46:6640–8.
- Shichang L, Wei Z, Song L, Wenfang S. A novel method for preparation of exfoliated UV-curable polymer/clay nanocomposites. *Eur Polym J.* 2008;44:1613–9.
- Fogelstrom L, Antoni P, Malmstrom E, Hult A. UV-curable hyperbranched nanocomposite coatings. *Prog Org Coat.* 2006;55:284–90.
- Keller L, Decker C, Zahouily K, Benfarhi S, Le Meins JM, Mieke-Brendle J. Synthesis of polymer nanocomposites by UV-curing of organoclay–acrylic resins. *Polymer.* 2004;45:7437–47.
- Owusu-Adom K, Allan Guymon C. Photopolymerization kinetics of poly(acrylate)–clay composites using polymerizable surfactants. *Polymer.* 2008;49:2636–43.
- Landry V, Riedi B, Blanchet P. Nanoclay dispersion effects on UV coatings curing. *Prog Org Coat.* 2008;62:400–8.
- Uhl FM, Webster DC, Davuluri SP, Wong SC. UV curable epoxy acrylate–clay nanocomposites. *Eur Polym J.* 2006;42:2596–605.
- Chartoff R. Thermal characteristics of thermosets formed by free radical photocuring. *J Therm Anal Cal.* 2006;85:213–7.
- Peila R, Lengvinaite S, Malucelli G, Priola A, Ronchetti S. Modified organophilic montmorillonites/LDPE nanocomposites. *J Therm Anal Cal.* 2008;91:107–11.
- Edwards G, Halley P, Kerven G, Martin D. Thermal stability analysis of organo-silicates, using solid phase microextraction techniques. *Thermochim Acta.* 2005;429:13–8.
- Leszczynska A, Pielichowski K. Application of thermal analysis methods for characterization of polymer/montmorillonite nanocomposites. *J Therm Anal Cal.* 2008;93:677–87.